3-2011

Delayed Wound Closure in Fibromodulin-Deficient Mice Is Associated with Increased TGF-β3 Signaling

Zhong Zheng

Calvin Nguyen

Xinli Zhang

Hooman Khorasani

Joyce Z. Wang

See next page for additional authors

Recommended Citation

Zheng, Z., Nguyen, C., Zhang, X., Khorasani, H., Wang, J. Z., Zara, J. N., Chu, F., Yin, W., Pang, S., Le, A., Ting, K., & Soo, C. (2011). Delayed Wound Closure in Fibromodulin-Deficient Mice Is Associated with Increased TGF-β3 Signaling. *Journal of Investigative Dermatology, 131* (3), 769-778. http://dx.doi.org/10.1038/jid.2010.381

At the time of publication, author Anh Le was affiliated with the University of Southern California. Currently, (s)he is a faculty member at the School of Dental Medicine at the University of Pennsylvania.

Delayed Wound Closure in Fibromodulin-Deficient Mice Is Associated with Increased TGF-β3 Signaling

Abstract

Fibromodulin (FMOD), a small leucine-rich proteoglycan, mediates scarless fetal skin wound repair through, in part, transforming growth factor-B (TGF-B) modulation. Using an adult fmod-null (fmod -/-) mouse model, this study further elucidates the interplay between FMOD and TGF-B expression during cutaneous repair and scar formation. Full-thickness skin wounds on fmod -/- and wild-type (WT) mice were closed primarily and analyzed. Histomorphometry revealed delayed dermal cell migration leading to delayed wound closure and significantly increased scar size in fmod -/- mice relative to WT, which was partially rescued by exogenous FMOD administration. In addition, fmod -/- wounds exhibited early elevation (within 24 hours post-wounding) of type I and type II TGF-B receptors as well as unexpectedly high fibroblast expression of TGF-B3, a molecule with reported antifibrotic and antimigratory effects. Consistent with elevated fibroblastic TGF-B3, fmod -/- fibroblasts were significantly less motile than WT fibroblasts. fmod -/- fibroblasts were also more susceptible to migration inhibition by TGF-B3, leading to profound delays in dermal cell migration. Increased scarring in fmod -/- mice indicates that TGF-B3's antimotility effects predominate over its antifibrotic effects when high TGF-B3 levels disrupt early fibroblastic wound ingress. These studies demonstrate that FMOD presence is critical for proper temporospatial coordination of wound healing events and normal TGF-B bioactivity. © 2011 The Society for Investigative Dermatology.

Keywords

EMTREE drug terms: collagen, fibromodulin, transforming growth factor beta receptor 1, transforming growth factor beta receptor 2, transforming growth factor beta3 EMTREE medical terms: animal cell, animal experiment, animal model, animal tissue, article, cell migration, controlled study, histopathology, male, migration inhibition, morphometrics, mouse, nonhuman, priority journal, scar formation, signal transduction, skin fibroblast, skin injury, wound closure, wound healing

Disciplines

Dentistry | Endodontics and Endodontology | Oral and Maxillofacial Surgery | Oral Biology and Oral Pathology | Periodontics and Periodontology

Comments

At the time of publication, author Anh Le was affiliated with the University of Southern California. Currently, (s)he is a faculty member at the School of Dental Medicine at the University of Pennsylvania.

Author(s)

Zhong Zheng, Calvin Nguyen, Xinli Zhang, Hooman Khorasani, Joyce Z. Wang, Janette N. Zara, Franklin Chu, Wei Yin, Shen Pang, Anh Le, Kang Ting, and Chia Soo

Delayed Wound Closure in Fibromodulin-Deficient Mice Is Associated with Increased TGF-β3 Signaling

Zhong Zheng[1], Calvin Nguyen[2], Xinli Zhang[2], Hooman Khorasani[3], Joyce Z. Wang[4], Janette N. Zara[5], Franklin Chu[6], Wei Yin[2,7], Shen Pang[1], Anh Le[8], Kang Ting[2] and Chia Soo[1]

Fibromodulin (FMOD), a small leucine-rich proteoglycan, mediates scarless fetal skin wound repair through, in part, transforming growth factor-β (TGF-β) modulation. Using an adult *fmod*-null (*fmod*$^{-/-}$) mouse model, this study further elucidates the interplay between FMOD and TGF-β expression during cutaneous repair and scar formation. Full-thickness skin wounds on *fmod*$^{-/-}$ and wild-type (WT) mice were closed primarily and analyzed. Histomorphometry revealed delayed dermal cell migration leading to delayed wound closure and significantly increased scar size in *fmod*$^{-/-}$ mice relative to WT, which was partially rescued by exogenous FMOD administration. In addition, *fmod*$^{-/-}$ wounds exhibited early elevation (within 24 hours post-wounding) of type I and type II TGF-β receptors as well as unexpectedly high fibroblast expression of TGF-β3, a molecule with reported antifibrotic and antimigratory effects. Consistent with elevated fibroblastic TGF-β3, *fmod*$^{-/-}$ fibroblasts were significantly less motile than WT fibroblasts. *fmod*$^{-/-}$ fibroblasts were also more susceptible to migration inhibition by TGF-β3, leading to profound delays in dermal cell migration. Increased scarring in *fmod*$^{-/-}$ mice indicates that TGF-β3's antimotility effects predominate over its antifibrotic effects when high TGF-β3 levels disrupt early fibroblastic wound ingress. These studies demonstrate that FMOD presence is critical for proper temporospatial coordination of wound healing events and normal TGF-β bioactivity.

Journal of Investigative Dermatology (2011) **131,** 769–778; doi:10.1038/jid.2010.381; published online 30 December 2010

INTRODUCTION

Transforming growth factor-βs (TGF-βs) are multifunctional cytokines with widespread effects on cell growth and differentiation, migration, and extracellular matrix (ECM) deposition, and have key roles in wound repair (Border *et al.*, 1992; Clark, 1996). With respect to cutaneous repair, TGF-β1 and TGF-β2 are known to promote fibroplasia and scar, while TGF-β3 may or may not reduce scar (Shah *et al.*, 1994, 1995; Murata *et al.*, 1997; Wu *et al.*, 1997; Occleston *et al.*, 2008; Ferguson *et al.*, 2009).

[1]*Department of Orthopaedic Surgery, University of California, Los Angeles, Los Angeles, California, USA;* [2]*School of Dentistry, University of California, Los Angeles, Los Angeles, California, USA;* [3]*Department of Dermatology, New York Medical College, Valhalla, New York, USA;* [4]*School of Medicine, University at Buffalo, Buffalo, New York, USA;* [5]*Department of Bioengineering, University of California, Los Angeles, Los Angeles, California, USA;* [6]*School of Dental Medicine, Tufts University, Boston, Massachusetts, USA;* [7]*Department of Endodontics and Periodontics, College of Stomatology, Dalian Medical University, Dalian, China and* [8]*Center for Craniofacial Molecular Biology, University of Southern California, Los Angeles, California, USA*

Correspondence: Chia Soo, Department of Orthopaedic Surgery, University of California, Los Angeles, MRL 2641A, Box 951759, 675 Charles E Young Drive, South, Los Angeles, California 90095-1759, USA.
E-mail: leozz95@gmail.com or Kang Ting, School of Dentistry, University of California, Los Angeles, Los Angeles, California, USA.
E-mail: kting@dentistry.ucla.edu

Abbreviations: ECM, extracellular matrix; FMOD, fibromodulin; QRT-PCR, quantitative reverse transcriptase-PCR; TGF, transforming growth factor; WT, wild-type

Received 23 July 2010; revised 16 October 2010; accepted 5 November 2010; published online 30 December 2010

The transition from scarless fetal-type repair to adult-type repair with scar occurs between days 16 (E16) and 18 (E18) of gestation in fetal rat skin (term = 21.5 days; Ihara *et al.*, 1990). Our previous results implicated decreased TGF-β1 and -β2, and increased TGF-β3 expression, as well as decreased type I and II TGF-β receptor (TβRI and TβRII) expression in scarless early gestation E16 fetal wounds (Soo *et al.*, 2003). Besides amplified TGF-β3, we also demonstrated significantly elevated fibromodulin (FMOD) protein induction as a potential mechanism for decreased scarring in E16 relative to E19 fetal wounds (Soo *et al.*, 2000). FMOD is a small leucine-rich proteoglycan that along with other small leucine-rich proteoglycans, such as decorin, can interact with a number of different cell surface receptors, cytokines, ECM components, and growth factors, such as TGF-β ligands to modulate their activity (Hildebrand *et al.*, 1994; Merline *et al.*, 2009). In a rat fetal model, we restored scarless repair to normally scarring E19 skin wounds by FMOD administration, whereas FMOD blockade by anti-FMOD antibodies induced scar in normally scarless E16 wounds (Soo *et al.*, 2001). Generally, scarless fetal repair coincided with relatively increased TGF-β3 and FMOD expression.

To further elucidate how FMOD modulates TGF-β signaling during wound repair, we used an adult *fmod*-null (*fmod*$^{-/-}$) mouse model. Unexpectedly, we demonstrated that rather than reduce scar, increased TGF-β3 in *fmod*$^{-/-}$ wounds inhibited initial dermal cell migration and postponed granulation tissue formation leading to delayed wound closure and increased scar size. Overall, FMOD absence

profoundly altered the normal temporospatial pattern of TGF-β ligand and receptor expression.

RESULTS

fmod$^{-/-}$ mice exhibit delayed dermal cell migration, delayed wound closure, and increased scar size

Coordinated epidermal and dermal cell migration into the wound was noted in wild-type (WT) wounds by day 1 post-injury (Figure 1a). WT wounds were closed (i.e., re-epithelialized) by day 3 with a small, shallow dermal concavity (Figure 1e). Surprisingly, epidermal migration in *fmod*$^{-/-}$ mice, which was distinctly observable at day 1 post-injury (Figure 1b), was not accompanied by dermal cell migration (Figure 1d and f). Deficient dermal cell migration and granulation tissue formation in *fmod*$^{-/-}$ mice created a bigger wound surface area requiring epithelial coverage relative to WT. This delayed wound closure as re-epithelialization was not complete in *fmod*$^{-/-}$ mice until day 5 post-injury and was accompanied by a large, deep, U-shaped dermal concavity or 'gap' extending from superficial dermis to subcutaneous fat (Figure 1j).

As *fmod*$^{-/-}$ and WT mice did not manifest any gross differences in wound closure tension or appearance (i.e., *fmod*$^{-/-}$ wound 'gap' visible only in histology sections; Figure 1f and h) and sutures were not removed until day 7, *fmod*$^{-/-}$ wound 'gap' cannot be explained by mechanical tension alone. As fibronectin promotes dermal fibroblast transmigration from a collagenous to fibrin clot or provisional matrix (Clark *et al*., 2003), we examined *fibronectin* messenger RNA (mRNA) expression in *fmod*$^{-/-}$ and WT mice. Quantitative reverse transcriptase-PCR (qRT-PCR) analysis revealed lower total wound *fibronectin* mRNAs in *fmod*$^{-/-}$ wounds compared with WT controls, wheras fibronectin levels were the same in unwounded *fmod*$^{-/-}$ and WT tissues (Supplementary Figure S1 online). These data are consistent with deficient dermal cell migration in *fmod*$^{-/-}$ animals. To determine if defects in epidermal motility may have contributed to delayed *fmod*$^{-/-}$ wound closure, we calculated the epidermal migration index (I_{EM}). Remarkably, I_{EM} was greater in *fmod*$^{-/-}$ wounds (directly down to the subcutaneous fat) than WT wounds (Figures 1e–j, 2a and b), indicating that wound closure delay was not due to retarded epidermal migration.

Interestingly, *fmod*$^{-/-}$ mice wounds that demonstrated minimal granulation tissue at the wound base at day 5 (Figure 1j), exhibited an exuberant fibroproliferative response with abundant granulation tissue formation and significantly higher wound fibroblast densities than WT wounds by day 7 (Supplementary Figure S2 online). The granulation tissue formed in *fmod*$^{-/-}$ mice, however, was markedly less vascular than WT, as evidenced by total wound capillary density (Suppplementary Figure S2 online). Meanwhile, exogenous FMOD administration to *fmod*$^{-/-}$ mice accelerated wound closure from days 5 to 4 post-injury (Figure 1i and m). Notably, FMOD application also prevented the larger scar phenotype in *fmod*$^{-/-}$ mice, restoring the scars to WT size (Figure 2c–h). Overall, *fmod*$^{-/-}$ mice exhibited an altered wound healing phenotype that was characterized by delayed dermal cell migration, delayed granulation tissue formation (Supplementary Figure S3 online), delayed wound closure (despite increased epidermal migration), decreased vascularity, and increased scar size.

fmod$^{-/-}$ fibroblasts and ECM exhibit significantly elevated TGF-β3 staining by day 0.5 post-injury

TGF-β3, when in the presence of high TβRII expression, has been described to inhibit human dermal fibroblast and endothelial cell migration and proliferation (Bandyopadhyay *et al*., 2006). To determine the effect of FMOD absence on TGF-β ligands, qRT-PCR and immunostaining was performed for TGF-β1, -β2, and -β3. Unwounded skin exhibited strong TGF-β3 staining in both the outer and basal layers of epidermis and hair follicles (Supplementary Figure S4 online), but TGF-β3 in WT and *fmod*$^{-/-}$ wounded epidermis and adjacent hair follicles dropped to negligible levels by day 0.5 post-injury (Figure 3a and b). At day 0.5 post-injury, no TGF-β3 staining was observed in WT mice ECM and only ~5% of fibroblasts exhibited TGF-β3 signals, and then only at minimal levels (Figure 3a). In marked contrast, *fmod*$^{-/-}$ mice displayed strong TGF-β3 signals in both the ECM and in ~25% of fibroblasts at day 0.5 post-injury (Figure 3b). Meanwhile, total dermal TGF-β3 protein expression in *fmod*$^{-/-}$ mice was also significantly higher at day 0.5 (Figure 3c). In addition, qRT-PCR analysis also revealed >10-fold higher total wound *tgf-β3* mRNAs in *fmod*$^{-/-}$ unwounded and day 0.5 post-injury wounds compared with WT controls (Figure 3d). Interestingly, *fmod*$^{-/-}$ mice exhibited relatively lower *tgf-β1* expression during the entire 14-day experimental period (Supplementary Figure S5 online), but higher dermal TGF-β1 staining at day 7 (not shown), while both TGF-β2 mRNA and dermal staining were transiently increased at 0.5 day after injury in *fmod*$^{-/-}$ mice (not shown). Thus, relative to TGF-β1 or -β2, TGF-β3 expression was markedly more altered in *fmod*$^{-/-}$ mice. The significant elevation of known antimigration factor, TGF-β3, may provide a mechanistic basis for delayed dermal cell migration in *fmod*$^{-/-}$ mice.

fmod$^{-/-}$ wounds with increased TβRI and TβRII protein staining

To determine if requisite TGF-β signaling receptors (Roberts and Sporn, 1996) are also upregulated in *fmod*$^{-/-}$ mice, qRT-PCR and immunostaining were performed for TβRI and TβRII; TβRII in particular is required for transducing antimigratory TGF-β3 signals (Bandyopadhyay *et al*., 2006). Strong TβRI staining was observed in *fmod*$^{-/-}$ dermal fibroblasts at the wound edge by day 0.5 post-injury (Figure 3F), while almost no TβRI staining was evident in day 0.5 WT dermal fibroblasts (Figure 3E). By day 1 post-injury, individual WT and *fmod*$^{-/-}$ fibroblasts exhibited strong TβRI signals (Figure 3g and h). However, numerically there were more fibroblasts with strong TβRI signals in *fmod*$^{-/-}$ than in WT wounds (Figure 3g and h), leading to significantly increased total dermal TβRI signals in *fmod*$^{-/-}$ wounds (Figure 3i). qRT-PCR analysis revealed a similar pattern of *tβrI* mRNA expression levels in unwounded WT and *fmod*$^{-/-}$ tissues (Figure 3j). *tβrI* mRNA of both WT and *fmod*$^{-/-}$ wounds peaked at day 0.5 post-injury, where *fmod*$^{-/-}$ *tβrI* transcript was ~1.84-fold higher than WT (Figure 3j).

TβRII staining, which was strong in both WT and *fmod*$^{-/-}$ epidermis before injury, was transiently but markedly

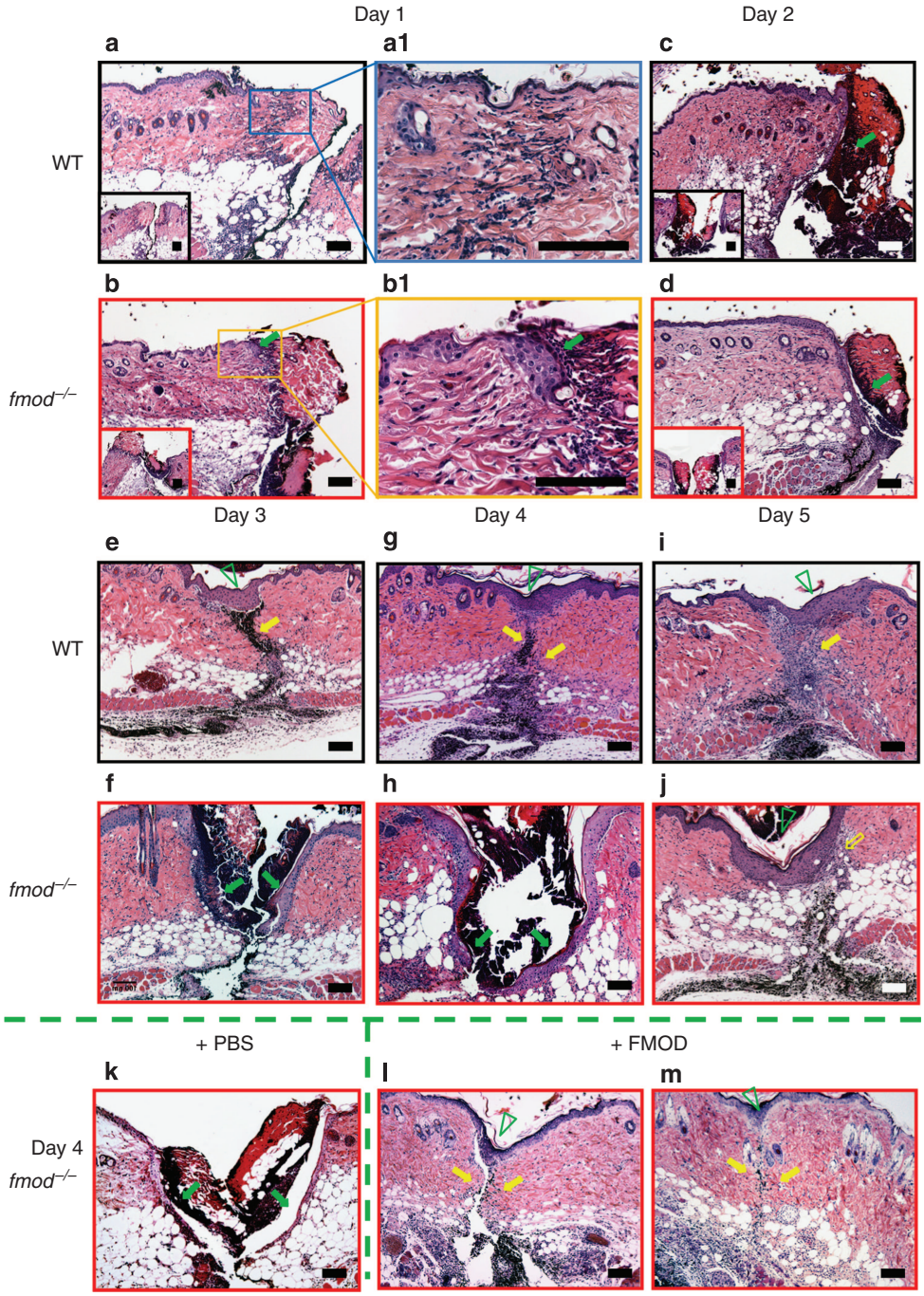

Figure 1. Hematoxylin and eosin staining of wild-type (WT) and *fmod*-null (*fmod*$^{-/-}$) skin wounds. At day 1, WT with minimal epidermal migration (**a**, **a1**); *fmod*$^{-/-}$ with significant migration (green arrow) (**b**, **b1**). At day 2, epidermal tongue (green arrow) present in WT (**c**) and *fmod*$^{-/-}$ mice (**d**). Insets in **a**–**d** show low magnification view of both wound edges. WT wound closed at day 3 with a deep concavity (green arrow) and granulation tissue (yellow arrow) (**e**, **g**, **i**). Deep concavity and absent granulation tissue (green arrows) in *fmod*$^{-/-}$ wound with epidermal migration to subcutaneous fat (green arrows; **f**, **h**, **j**). Epithelial hypertrophy present in WT and *fmod*$^{-/-}$ wounds (green arrows) (**i**, **j**). *fmod*$^{-/-}$ wound at 4 days after control phosphate-buffered saline (PBS) (**k**; green arrows show migrating epidermis). Fibromodulin (FMOD) accelerated *fmod*$^{-/-}$ wound closure (green arrows) and promoted granulation tissue (yellow arrows; **l**, **m**). Bar = 100 μm.

downregulated to negligible levels in WT wound edges at day 0.5 and day 1 post-injury (Figure 3k and m). Meanwhile, TβRII signals in age-matched *fmod*$^{-/-}$ wound edge epidermis and hair follicles were unchanged from strong pre-injury levels (Figure 3l and n; Supplementary Figure S4, E and F online). Intriguingly, TβRII signals were negligible in WT fibroblasts at day 0.5 (Figure 3k), while *fmod*$^{-/-}$ fibroblasts exhibited moderate TβRII signals (Figure 3l) that increased to strong signals by day 1 (Figure 3n), when WT fibroblasts exhibited only moderate staining (Figure 3m). These data demonstrate that like TβRI, *fmod*$^{-/-}$ fibroblasts express significantly more TβRII protein than WT fibroblasts

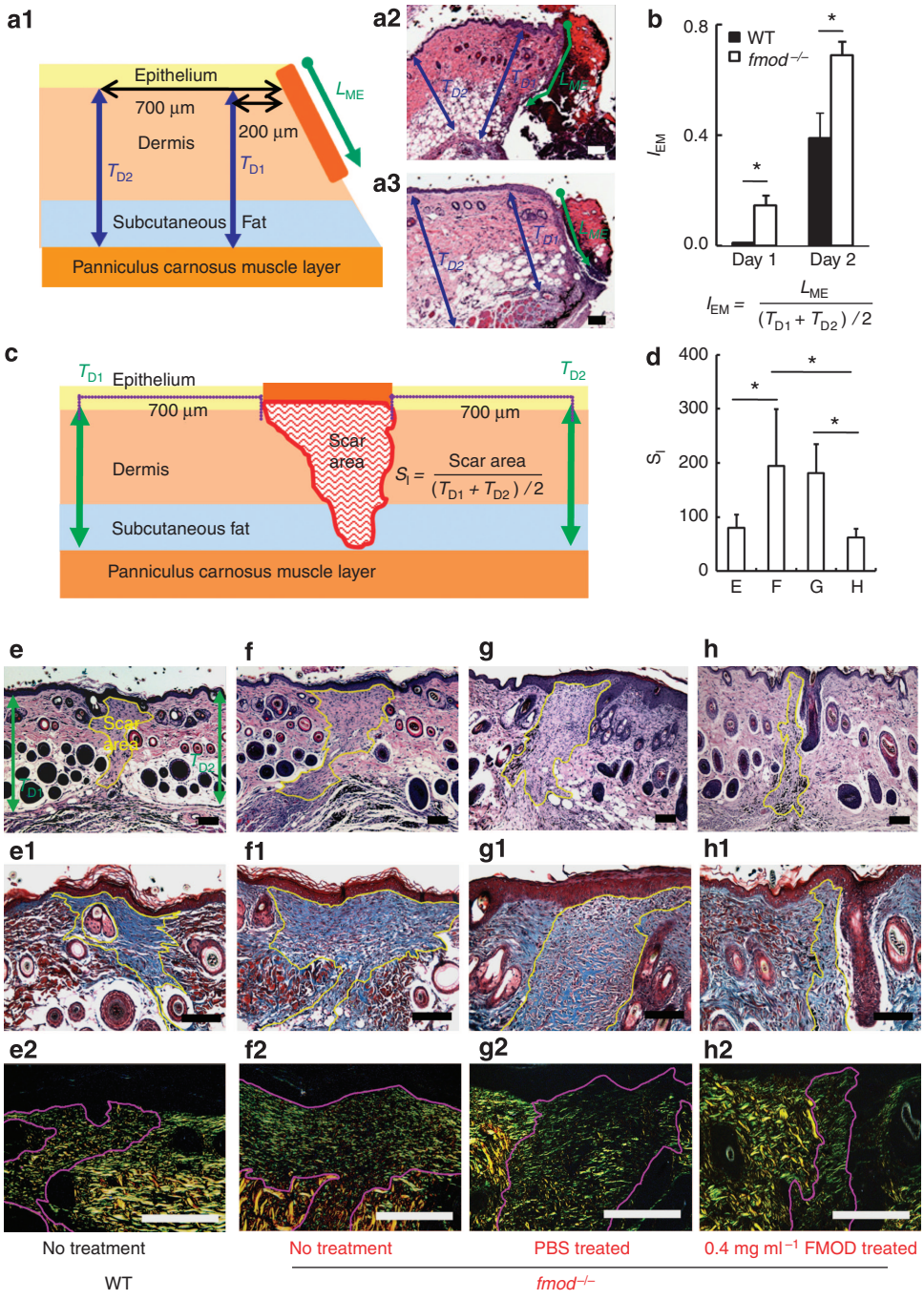

Figure 2. Determination of epidermal migration index (I_{EM}) and scar size index (S_I). Schematic (**a1**) and corresponding hematoxylin and eosin (H and E) images (**a2** and **a3**) illustrating the measurements used for I_{EM}. Tissue thickness measurements at 200 μm (T_{D1}) and 700 μm (T_{D2}) from the wound or scar edge (blue arrows) were obtained using Image-Pro Plus 6.0. (**b**) I_{EM} at days 1 and 2 post-injury ($N=8$). Schematic (**c**) and corresponding Hand E image (**d**) illustrating the measurements used for S_I at day 14 post-injury ($N=16$). At day 14 post-injury, *fmod*$^{-/-}$ mice exhibited larger scar phenotypes (**f**; scar area outlined in yellow) compared with WT (**e**) that were rescued by fibromodulin (FMOD) application (**h**), but not phosphate-buffered saline (PBS) control (**g**). Masson's trichrome staining (**e1**–**h1**; scar area outlined in purple) and Picro-sirius red staining with polarized light (**e2**–**h2**) are also shown. Significant differences ($P<0.05$) are marked with asterisks. Bar = 100 μm.

in the initial day 0.5 to day 1 post-injury (Figure 3o). Thus, acute injury elicits a significantly more robust TGF-β3 and TβRI/TβRII response in *fmod*$^{-/-}$ dermal cells, which further supports elevated TGF-β3 activity as the mechanism for delayed dermal cell migration in *fmod*$^{-/-}$ wounds.

fmod$^{-/-}$ fibroblasts exhibit decreased migration and collagen expression

To determine if *fmod*$^{-/-}$ dermal fibroblasts exhibit delayed migration—and if this delay is influenced by TGF-β3—primary *fmod*$^{-/-}$ and WT mice skin fibroblasts were isolated for cell migration assays. Compared with WT, *fmod*$^{-/-}$

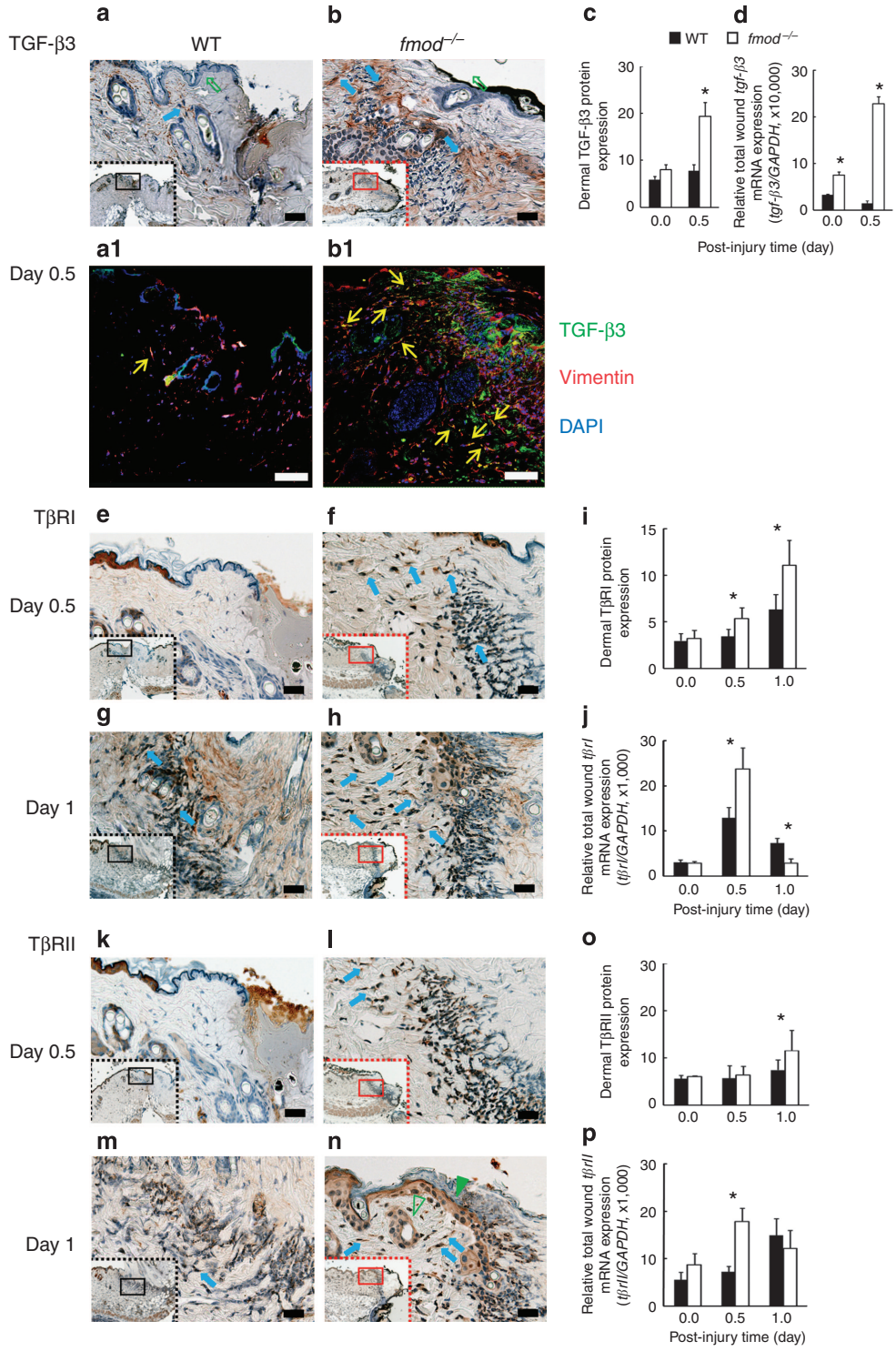

Figure 3. Immunohistochemistry (IHC) of transforming growth factor (TGF)-β3 (a–b), TβRI (e–h), and TβRII (k–n) expression in wild-type (WT) and *fmod*$^{-/-}$ mice skin wounds. Evaluation of the staining was focused on epidermis (green arrows) and hair follicle (green open triangle) adjacent to the wound, migrating epidermal tongue (green solid triangle) as well as dermal fibroblasts (blue arrows) and ECM in the wound area. Under confocal microscopy (**a1**, **b1**), dermal fibroblasts are identified by positive vimentin immunostaining (red) with general nucleus counter staining (4′,6-diamidino-2-phenylindole (DAPI)) in blue. Dermal fibroblasts (vimentin-positive cells) co-expressing TGF-β3 (green) are indicated by yellow arrows (**a1**–**b1**). Computerized quantitation of dermal protein expression (TGF-β3, **c**; TβRI, **i**; and TβRII, **o**; $N = 9$) is shown. Relative total wound mRNA expression (TGF-β3, **d**; TβRI, **j**; and TβRII, **p**; $N = 4$) are also presented to confirm the IHC evaluation. Significant differences ($P < 0.05$) are marked with asterisks. Bar = 25 μm.

fibroblasts demonstrated significantly less motility in collagen matrices (56% compared with WT dermal fibroblasts; Figure 4a). Exogenous FMOD protein restored *fmod*$^{-/-}$ fibroblast migration to phosphate-buffered saline-treated WT levels, confirming that FMOD absence was responsible for decreased *fmod*$^{-/-}$ fibroblast migration (Figure 4a). Meanwhile, addition of up to 200 nM FMOD protein did not affect WT fibroblast migration (Figure 4). Interestingly, 100 pM TGF-β1 also restored *fmod*$^{-/-}$ fibroblast migration to phosphate-buffered saline-treated WT levels, while TGF-β1 significantly increased dermal fibroblast migration in WT cells (Figure 4a). Remarkably, combination of FMOD/TGF-β1 increased *fmod*$^{-/-}$ and WT dermal fibroblast migration to 236 and 182%, respectively, above phosphate-buffered saline controls (Figure 4a). These results show that deficient migration in *fmod*$^{-/-}$ fibroblasts can be overcome by exogenous FMOD or TGF-β1 and, excitingly, that FMOD augments TGF-β1 pro-motility effects in both *fmod*$^{-/-}$ and WT fibroblasts.

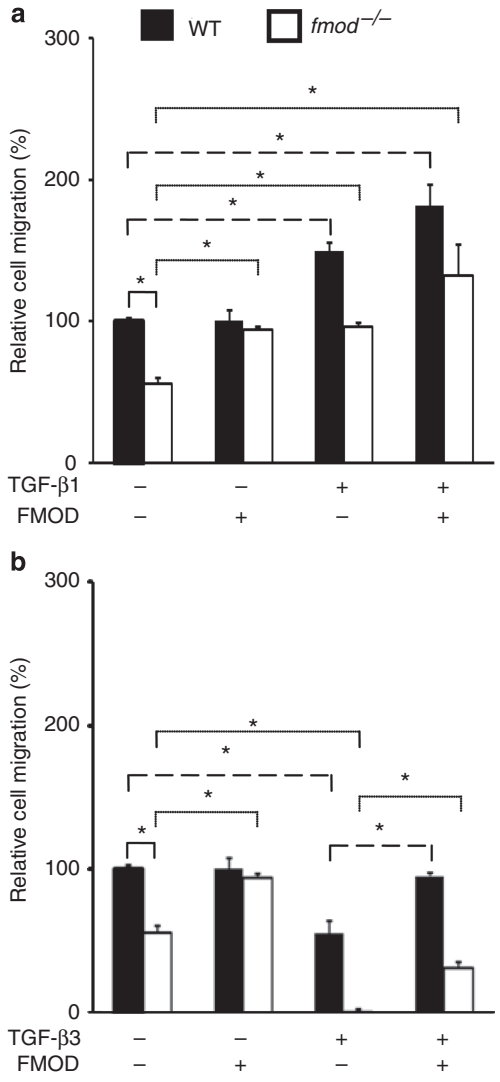

Figure 4. *In vitro* migration assay of primary dermal fibroblasts derived from adult wild-type (WT) and *fmod*$^{-/-}$ adult mice skin. (**a**) Fibromodulin (FMOD; 200 nM FMOD) and/or transforming growth factor (TGF)-β1 (100 pM TGF-β1); (**b**) FMOD (200 nM FMOD) and/or TGF-β3 (100 pM TGF-β3). Data are means of three independent experiments with four replica wells for each experiment. Statistically significant differences ($P<0.05$) are marked with asterisks.

An elegant series of studies by Bandyopadhyay *et al.* (2006) established that high TGF-β3 and high TβRII co-expression inhibited migration of human cells, such as dermal fibroblasts and endothelial cells. To directly determine if high TGF-β3 inhibits mouse dermal fibroblast motility and if this inhibitory effect can be modulated by FMOD, both WT and *fmod*$^{-/-}$ fibroblast migration response to TGF-β3 were assayed (Figure 4b). Consistent with results from Bandyopadhyay *et al.* (2006), 100 pM TGF-β3 significantly inhibited WT fibroblast migration, but surprisingly, TGF-β3 entirely inhibited *fmod*$^{-/-}$ fibroblasts migration (Figure 4b). Furthermore, FMOD addition completely prevented TGF-β3-mediated inhibition of WT fibroblast migration and partially prevented TGF-β3-mediated inhibition of *fmod*$^{-/-}$ fibroblast migration (Figure 4b). These data indicate that antimotility effects of TGF-β3 are attenuated by the presence of FMOD and that *fmod*$^{-/-}$ fibroblasts are particularly susceptible to migratory inhibition by TGF-β3. Collectively, increased dermal TGF-β3 signaling, increased fibroblastic susceptibility to antimigratory TGF-β3 effects, and decreased *in vitro* fibroblast migration provide a mechanism for delayed dermal cell migration in *fmod*$^{-/-}$ wounds.

TGF-β3 has well-described scar reduction properties (Shah *et al.*, 1994, 1995; Occleston *et al.*, 2008), as well as documented ability to block TGF-β1-induced type I procollagen α2 and type III procollagen α1 transcription (Murata *et al.*, 1997). To determine if decreased fibroblast synthetic function also contributed to the initial lack of granulation tissue deposition in *fmod*$^{-/-}$ wounds, we analyzed type I and III mRNA expression in WT versus *fmod*$^{-/-}$ wounds (Supplementary Figure S6 online). Surprisingly, when normalized to glyceraldehyde-3-phosphate dehydrogenase on an individual cell basis, *fmod*$^{-/-}$ wounds exhibited significantly less type I and III transcripts relative to WT not only in the first 12–48 hours after injury, but also even during the exuberant fibroplasia phase at day 7 (Supplementary Figure S2 online). However, although individual *fmod*$^{-/-}$ fibroblasts produced less collagen *per se*, the total number of dermal cells—which were primarily fibroblasts—was significantly greater in *fmod*$^{-/-}$ wounds by day 7 after injury (Supplementary Figure S2 online). Thus, by day 7, the scar size and the collective amount of collagen produced were overall greater in *fmod*$^{-/-}$ wounds than in WT. These data demonstrate that decreased migration and collagen production by *fmod*$^{-/-}$ fibroblasts can account for the early delay in dermal cell migration and granulation tissue formation in *fmod*$^{-/-}$ wounds that contribute to increased scar size.

DISCUSSION

FMOD, as well as other small leucine-rich proteoglycans such as decorin and biglycan, can bind all three TGF-β isoforms with variable affinity to modulate their bioactivity. Our previous reports described an increase in FMOD and TGF-β3 levels in early gestation scarless fetal wounds

(Soo *et al.*, 2000, 2003), while exogenous FMOD administration prevented scar formation in late gestation scarring fetal wounds (Soo *et al.*, 2001). In addition, Stoff *et al.* (2007) demonstrated that adenoviral FMOD overexpression reduced scar size in rabbit primary closure wounds. In this study, we used an adult *fmod*$^{-/-}$ mouse model to further elucidate how FMOD modulates TGF-β signaling during cutaneous wound repair.

Remarkably, a single missing gene, *fmod,* led to marked alterations in wound healing phenotype and in TGF-β ligand and receptor expression with elevated TβRI and TβRII levels, as well as unexpectedly high TGF-β3 levels in fibroblasts. Cellular events such as dermal cell migration and granulation tissue formation were all profoundly delayed in *fmod*$^{-/-}$ mice. This delay increased the total wound surface area in *fmod*$^{-/-}$ mice relative to WT, and required longer times for wound closure through re-epithelialization (Figure 5).

Phenotypically, delayed cellular entry in wounds is also apparent in other cutaneous healing models with altered TGF-β signaling (Crowe *et al.*, 2000; Denton *et al.*, 2009). However, in our model, delayed cellular wound entry was not associated with specific deletion of TGF-β ligands or receptors, but rather absence of *fmod* only. In fact, *fmod*$^{-/-}$ mice exhibited similar or higher TGF-β ligand and receptor staining levels compared with WT. This indicates that FMOD is a critical component of normal TGF-β signaling during the wound healing process.

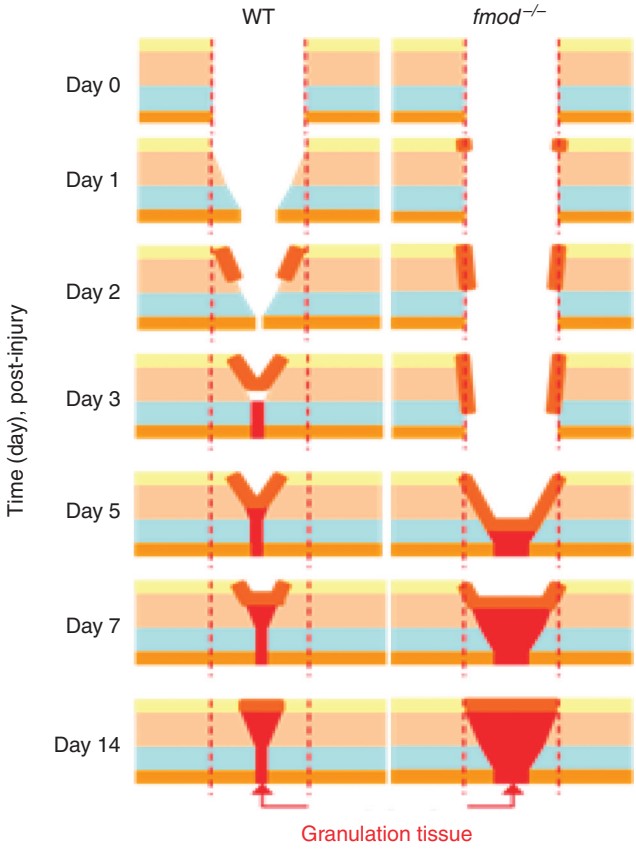

Figure 5. Schematic illustrating the different wound healing processes of wild-type (WT) and *fmod*$^{-/-}$ adult mice.

Another important finding is the association of high TGF-β3 levels with increased wound surface area and scar size in adult *fmod*$^{-/-}$ mice. We show that excessive TGF-β3 during the early cell migration phase preceding fibroplasia unexpectedly leads to increased scar formation through mechanisms related to delayed dermal cell migration (Bandyopadhyay *et al.*, 2006) and delayed granulation tissue formation through known ability of TGF-β3 to block TGF-β1-induced type I and III mRNA (Murata *et al.*, 1997). This then leads to an excessively exuberant fibroproliferative response by day 7 that results in a larger scar in *fmod*$^{-/-}$ wounds. These studies suggest that antifibrotic TGF-β3 effects are more optimally used during the fibroplasia phase of repair, rather than during early wound healing when TGF-β3's inhibitory effects on dermal cell migration may outweigh any potential antifibrotic benefits.

Excitingly, TGF-β3 (Avotermin (Juvista), Renovo, Manchester, UK) is currently in phase III clinical trials for scar revision surgery in the United States and Europe (http://www.renovo.com). TGF-β3 injected intradermally immediately after and at 24 hours post-surgery appears to effectively decrease the appearance of scars by visual assessment (Ferguson *et al.*, 2009). This raises obvious questions of how early elevated TGF-β3 levels in adult *fmod*$^{-/-}$ mice increase scar, while early TGF-β3 application in humans appears to decrease scar formation, and also how high TGF-β3 levels are associated with scarless repair in fetal skin (Soo *et al.*, 2003; Chen *et al.*, 2005). One possible answer is that high exogenous TGF-β3 administration in the presence of normal, albeit low, WT wound FMOD levels (Soo *et al.*, 2000) in mice or humans does not significantly inhibit TGF-β1-mediated cell migration—and therefore does not retard wound healing. Furthermore, early TGF-β3 application may effectively compete with TGF-β1 for TβRII binding, leading to decreased TGF-β1 signaling and decreased AP-1-mediated TGF-β1 autoinduction during the fibroplasia phase (Kim *et al.*, 1990). In this scenario, TGF-β3 modulation of profibrotic TGF-β1 effects decreases overall scar, while antimigratory TGF-β3 effects are dampened by normal FMOD levels.

With respect to the high TGF-β3 levels observed in scarless fetal wounds, it is noteworthy that TGF-β3 promotes rather than inhibits mesenchymal cell migration in fetal animals through tenascin-mediated mechanisms (Kohama *et al.*, 2002). In addition, fetal fibroblasts also demonstrate a delayed response to TGF-β3 (Rolfe *et al.*, 2007)—perhaps making them less susceptible to antimigratory TGF-β3 effects. Consistent with this, TβRII levels were detected in late gestation scarring E19 wounds as early as 12 hours after injury, but no TβRII staining was detected in early gestation scarless E16 wounds until 48 hours after injury (Soo *et al.*, 2003). Thus, E16 wounds may be significantly less responsive to antimigratory TGF-β3 effects as TβRII presence is required for TGF-β3 inhibition of migration (Bandyopadhyay *et al.*, 2006).

Meanwhile high TGF-β3 downregulates TβRI in fetal rat cranial sutures (Opperman *et al.*, 2002), but not in fetal rat

skin wounds (Soo *et al.*, 2003) or as we have shown here, in adult *fmod*$^{-/-}$ mice skin wounds. These data indicate that cellular responses to TGF-β3 are contextually dependent on development stage, cell type, and differentiation state and significantly on the presence or absence of FMOD. Taken together, our data raise intriguing questions of whether early FMOD application to decrease overall wound size by promoting more rapid dermal cell migration and initial wound contracture, combined with later TGF-β3 application to decrease overall ECM deposition during the fibroplasia phase, may be even more efficacious than TGF-β3 alone.

Interestingly, exogenous FMOD administration did not completely overcome delayed wound closure and delayed granulation tissue formation caused by *fmod* gene deficiency. This suggests that one-time FMOD application is insufficient to overcome the effects of prolonged FMOD deficiency. We are currently testing whether sustained FMOD administration before wounding will restore normal skin repair and TGF-β expression patterns to *fmod*$^{-/-}$ wounds.

An additional finding in this study is that FMOD interacts differently with different TGF-β ligands; FMOD dampens TGF-β3-mediated antimotility effects while augmenting TGF-β1-induced pro-motility effects. Thus, despite similar early expression of TGF-β1 in WT and *fmod*$^{-/-}$ wounds, there is a profound lack of early dermal fibroblast migration in *fmod*$^{-/-}$ wounds—likely due to absent pro-migratory factors (e.g., lack of FMOD to augment TGF-β1 pro-motility effects) coupled with excessive antimigratory factors (e.g., high TGF-β3 and TβRII expression and lack of FMOD to block TGF-β3 antimotility effects). These results demonstrate that FMOD is a critical *in vivo* modulator of TGF-β bioactivity, governing timely dermal cell migration and granulation tissue formation in the wound bed.

One limitation of the *fmod*$^{-/-}$ mouse model is that non-conditional global FMOD tissue deficiency will elicit adaptive changes that may confound the precise dissection of FMOD's function in specific cell types during wound healing. For instance, consistent with described compensatory upregulation of *lumican* expression in *fmod*$^{-/-}$ mice tendons (Svensson *et al.*, 1999), we found compensatory *lumican*, *decorin*, and *biglycan* upregulation in unwounded *fmod*$^{-/-}$ mice skin (data not shown). We anticipate that the application of selective *fmod* disruption through inducible, lineage-specific *fmod* deletion models, such as that described for TβRII (Denton *et al.*, 2009), or *fmod* siRNA approaches will further aid our understanding of this important small leucine-rich proteoglycan.

MATERIALS AND METHODS

Wound generation

All experiments were performed under institutionally approved protocols provided by Chancellor's Animal Research Committee at UCLA (protocol number: 2000-058-21). Three and one-half month old male WT and *fmod*$^{-/-}$ mice (Svensson *et al.*, 1999) were anesthetized and the dorsal skin was sterilely prepared. Four, full thickness, 10 × 3 mm skin ellipses with the underlying panniculus carnosus muscle were excised on each mice. Each open wound edge was injected with 25-μl phosphate-buffered saline or 0.4 mg ml^{-1} recombinant FMOD solution (25 μl × 2 edges = 50 μl total per wound) (Supplementary Figure S7 online). Wounds were then closed primarily with 4-0 Nylon using two simple interrupted sutures consistently placed at one-third intervals in each 10 mm length wound. All wounds were separated by at least 2 cm to minimize adjacent wound effects. Sutures were removed at day 7 post-injury and wounds were harvested at 0.5, 1, 2, 3, 5, 7, and 14 days after injury (12–16 separate animals for each time point; $N = 24$–36 wounds per time point). Unwounded skin from identical locations in three animals were collected as controls. Tissue for RNA isolation (entire wound + 1 mm edge) was immediately frozen in liquid nitrogen and stored at −80 °C until RNA extraction. Wound tissue for histology (entire wound + 10 mm edge) was bisected centrally, between the two 4-0 Nylon sutures and perpendicular to the long axis of each 10 mm length wound and placed in formalin.

Histology

After fixation, sample skins were dehydrated, paraffin-embedded, and cut into 5-μm sections for hematoxylin and eosin staining. To ensure consistent sampling from the center rather than the periphery of the wound, specimens were sectioned starting from the areas of previous wound bisection.

In reviewing the literature, we did not come across any well-described methodologies for quantifying epidermal migration or total scar size in primary intention wounds. Thus, to standardize measurements of epidermal migration relative to different wounds from different animals for this study, we describe below I_{EM}, which is determined by:

$$I_{EM} = \frac{L_{ME}}{(T_{D1} + T_{D2}/2)}$$

Total migrating epidermal length (L_{ME}) from the wound edge was obtained using Image-Pro Plus 6.0 (Media Cybernetics, Bethesda, MD; Figure 2a1). To normalize for skin thickness variability among different animals, L_{ME} measurements were divided by average dermal + subcutaneous fat thickness (T_D; defined as the distance between the epidermal–dermal junction down to the panniculus carnosus). In order to quantitatively show the differences in scar or granulation tissue formation between primarily closed WT and *fmod*$^{-/-}$ mouse wounds, we created the scar index (S_I), whereby the total scar area is divided by the average dermal thickness (Figure 2c):

$$S_I = \frac{\text{Scar area}}{(T_{D1} + T_{D2})/2}$$

To ensure consistency, scar area measurements were taken from the bisected tissue specimens at the wound center and extended to the panniculus carnosus (Khorasani *et al.*, 2010).

Immunohistochemistry

Immunohistochemistry staining was performed as previously described (Soo *et al.*, 2003). Antibodies used in this study are listed in Supplementary Table S1 online. Computerized immunolocalization intensity analysis was performed using commercial software Image-Pro Plus 6.0. Relative dermal protein expression was quantitated by the mean optical density of staining signal × percent area positively stained × 100 (Allen and Southern, 2002). Confocal immunofluorescence images were taken on a confocal microscope

(Leica TCS-SP, Allendale, NJ). Fibroblasts were identified and quantitated by vimentin immunostaining.

qRT-PCR

Expression of messenger RNA (mRNA) was measured by qRT-PCR using TaqMan Gene Expression Assays (Supplementary Table S2 online) on a 7500 Fast Real-Time PCR system (Applied Biosystems, Foster City, CA). Concomitant glyceraldehyde-3-phosphate dehydrogenase was also performed in separate tubes for each RT reaction with TaqMan Rodent glyceraldehyde-3-phosphate dehydrogenase control reagents. For each gene, at least three separate sets of qRT-PCR analyses were performed from different complementary DNA templates.

Dermal fibroblast migration assay

Primary dermal fibroblasts from WT and *fmod*$^{-/-}$ adult mice were derived and maintained as described by Denton *et al.* (2009). Cell migration assays were performed in 24-well tissue culture plates using HTS Fluoroblok inserts with 8 mm pore size Fluorescence Blocking PET track-etched membranes (Becton Dickinson Labware, Franklin Lakes, NJ; Tamura *et al.*, 1999; De Wever *et al.*, 2004; White *et al.*, 2005). Upper surfaces of the inserts were coated with 200 ml collagen matrices (Mierke *et al.*, 2010), rinsed with DMEM (Invitrogen, Carlsbad, CA), and placed into 24-well tissue culture plates containing 500 µl of invasion buffer (DMEM + 0.5% fetal bovine serum (Invitrogen)) combined with 100 pM TGF-β1 or TGF-β3 (Sigma, St Louis, Mo) and/or 200 nM recombinant FMOD per well. After 16-hours serum starvation, passage 3 fibroblasts in 100 µl of invasion buffer were added to each insert chamber and allowed to invade toward the underside of the membrane for 48 hours. Non-invading cells were removed by wiping the upper side of the membrane with a cotton swab. Invaded cells were fixed and stained with 0.4 mg ml^{-1} 4′,6-diamino-2-phenylindole (Sigma) before counting (Tamura *et al.*, 1999; De Wever *et al.*, 2004; White *et al.*, 2005).

Statistical analysis

The results are graphically depicted as the mean ± SD. *T*-test was used to assess statistical significance between study groups using SPSS software (13.0 for Windows, SPSS, Chicago, IL). *P*-value <0.05 was considered statistically significant.

CONFLICT OF INTEREST

Drs Zheng, Ting, and Soo are inventors on FMOD-related patents. Drs Ting and Soo are founders of Scarless Laboratories, a company that is assigned and/or intends to license FMOD in related patents.

ACKNOWLEDGMENTS

This study was supported by the Wunderman Family Foundation, the Plastic Surgery Research Foundation, and R21 DE015118-01. *fmod*$^{-/-}$ animals were kindly provided by Dr Ake Oldberg (Lund, Sweden; Svensson *et al.*, 1999). We thank Dr Grace Xinlian Chang from the UCLA Department of Surgery for assistance with animal surgeries.

SUPPLEMENTARY MATERIAL

Supplementary material is linked to the online version of the paper at http://www.nature.com/jid

REFERENCES

Allen A, Southern S (2002) A novel technique of computer-assisted image analysis to quantify molecular stress in cetaceans. (http://www.mediacy.com/pdfs/021209cetaceans.pdf)

Bandyopadhyay B, Fan J, Guan S *et al.* (2006) A 'traffic control' role for TGF-β3: orchestrating dermal and epidermal cell motility during wound healing. *J Cell Biol* 172:1093–105

Border WA, Noble NA, Yamamoto T *et al.* (1992) Natural inhibitor of transforming growth factor-beta protects against scarring in experimental kidney disease. *Nature* 360:361–4

Chen W, Fu XB, Ge SL *et al.* (2005) Ontogeny of expression of transforming growth factor-beta and its receptors and their possible relationship with scarless healing in human fetal skin. *Wound Repair and Regeneration* 13:68–75

Clark R (1996) Wound repair: overview and general considerations. In: *The Molecular and Cellular Biology of Wound Repair* (Clark R, ed). New York: Plenum Press, 3–50

Clark RAF, An JQ, Greiling D *et al.* (2003) Fibroblast migration on fibronectin requires three distinct functional domains. *J Invest Dermatol* 121:695–705

Crowe MJ, Doetschman T, Greenhalgh DG (2000) Delayed woundhealing in immunodeficient TGF-β1 knockout mice. *J Invest Dermatol* 115:3–11

De Wever O, Westbroek W, Verloes A *et al.* (2004) Critical role of N-cadherin in myofibroblast invasion and migration *in vitro* stimulated by colon-cancer-cell-derived TGF-β or wounding. *J Cell Sci* 117:4691–703

Denton CP, Khan K, Hoyles RK *et al.* (2009) Inducible lineage-specific deletion of TβRII in fibroblasts defines a pivotal regulatory role during adult skin wound healing. *J Invest Dermatol* 129:194–204

Ferguson M, Duncan J, Bond J *et al.* (2009) Prophylactic administration of avotermin for improvement of skin scarring: three double-blind, placebo-controlled, phase I/II studies. *Lancet* 373:1264–74

Hildebrand A, Romaris M, Rasmussen L *et al.* (1994) Interaction of the small interstitial proteoglycans biglycan, decorin and fibromodulin with transforming growth factor β. *Biochem J* 302:527–34

Ihara S, Motobayashi Y, Nagao E *et al.* (1990) Ontogenic transition of wound-healing pattern in rat skin occurring at the fetal stage. *Development* 110:671–80

Khorasani H, Zheng Z, Nguyen C *et al.* (2010) A quantitative approach to scar analysis. *Am J Pathol* (in press)

Kim SJ, Angel P, Lafyatis R *et al.* (1990) Autoinduction of transforming growth factor-beta-1 is mediated by the Ap-1 complex. *Mol Cell Biol* 10:1492–7

Kohama K, Nonaka K, Hosokawa R *et al.* (2002) TGF-beta-3 promotes scarless repair of cleft lip in mouse fetuses. *J Dental Res* 81:688–94

Merline R, Lazaroski S, Babelova A *et al.* (2009) Decorin deficiency in diabetic mice: aggravation of nephropathy due to overexpression of profibrotic factors, enhanced apoptosis and mononuclear cell infiltration. *J Physiol Pharmacol* 60(Suppl 4):5–13

Mierke CT, Kollmannsberger P, Zitterbart DP *et al.* (2010) Vinculin facilitates cell invasion into three-dimensional collagen matrices. *J Biol Chem* 285:13121–30

Murata H, Zhou L, Ochoa S *et al.* (1997) TGF-β3 stimulates and regulates collagen synthesis through TGF-β1-dependent and independent mechanisms. *J Invest Dermatol* 108:258–62

Occleston NL, Laverty HG, O'Kane S *et al.* (2008) Prevention and reduction of scarring in the skin by transforming growth factor beta 3 (TGFbeta3): from laboratory discovery to clinical pharmaceutical. *J Biomater Sci Polym Ed* 19:1047–63

Opperman LA, Moursi AM, Sayne JR *et al.* (2002) Transforming growth factor-beta 3 (Tgf-beta 3) in a collagen gel delays fusion of the rat posterior interfrontal suture *in vivo*. *Anat Rec* 267:120–30

Roberts A, Sporn M (1996) Transforming grough factor-β. In: *The Molelular and Cellular Biology of Wound Repair* (Clark R, ed), New York: Plenum Press, 275–308

Rolfe KJ, Richardson J, Vigor C *et al.* (2007) A role for TGF-beta 1-induced cellular responses during wound healing of the non-scarring early human fetus? *J Invest Dermatol* 127:2656–67

Shah M, Foreman D, Ferguson M (1994) Neutralising antibody to TGF-β1,2 reduces cutaneous scarring in adult rodents. *J Cell Biol* 107: 1137–57

Shah M, Foreman D, Ferguson M (1995) Neutralisation of TGF-β1, and TGF-β2 or exogenous addition of TGF-β3 to cutaneous rat wounds reduces scarring. *J Cell Sci* 108:985–1002

Soo C, Beanes S, Dang C *et al.* (2001) Fibromodulin, a TGF-β modulator, promotes scarless fetal repair. *Surgical Forum* 2001:578–81

Soo C, Beanes SR, Hu F-Y *et al.* (2003) Ontogenetic transition in fetal wound transforming growth factor-β regulation correlates with collagen organization. *Am J Pathol* 163:2459–76

Soo C, Hu F, Zhang X *et al.* (2000) Differential expression of fibromodulin, a transforming growth factor-β modulator, in fetal skin development and scarless repair. *Am J Pathol* 157:423–33

Stoff A, Rivera AA, Mathis JM *et al.* (2007) Effect of adenoviral mediated overexpression of fibromodulin on human dermal fibroblasts and scar formation in full-thickness incisional wounds. *J Mol Med* 85:481–96

Svensson L, Aszodi A, Reinholt F *et al.* (1999) Fibromodulin-null mice have abnormal collagen fibrils, tissue organization, and altered lumican deposition in tendon. *J Biol Chem* 274:9636–47

Tamura M, Gu J, Takino T *et al.* (1999) Tumor suppressor PTEN inhibition of cell invasion, migration, and growth: differential involvement of focal adhesion kinase and $p130^{Cas}$. *Can Res* 59:442–9

White ES, Atrasz RG, Dickie EG *et al.* (2005) Prostaglandin E_2 inhibits fibroblast migration by E-prostanoid 2 receptor-mediated increase in PTEN Activity. *Am J Resp Cell Mol Biol* 32:135–41

Wu LC, Siddiqui A, Morris DE *et al.* (1997) Transforming growth factor beta 3 (TGF beta 3) accelerates wound healing without alteration of scar prominence – Histologic and competitive reverse-transcription polymerase chain reaction studies. *Arch Surg-Chicago* 132: 753–60